Study and Comparison of the Performance of Steel Frames with BRB and SMA Bracing

Mohsen Jalalvandi

Ahmad Soraghi

Seyed Mohammadreza Farooghi Mehr

Abbas Haghollahi

Ali Abasi

Study and Comparison of the Performance of Steel Frames with BRB and SMA Bracing

Mohsen Jalalvandi,[1] Civ. Eng.; Ahmad Soraghi,[2] Dr.;
S. Mohammadreza Farooghi-Mehr,[3] Civ. Eng.;
Abbas Haghollahi,[1] Dr; & Ali Abasi,[4] Civ. Eng.

1 Department of Civil Engineering, Shahid Rajaee Tarbiat Modares University, Tehran, Iran
2 Department of Civil Engineering, University of Akron, Akron, Ohio, USA and Bureau Veritas, Los Angeles, California, USA
3 Department of Civil and Environmental Engineering, University of Nebraska–Lincoln, Lincoln, Nebraska, USA
4 Department of Civil and Environmental Engineering, Western University, London, Ontario, Canada

Correspondence — Ahmad Soraghi, *email* as481@1870.uakron.edu.

ORCID Ahmad Soraghi http://orcid.org/0000-0001-8582-0347

Abstract

Designing steel structures with Concentric Braced Frame (CBF) lateral systems has been common in recent decades. This type of bracing has a quite unstable and complicated behavior in relatively intense earthquakes. This study tries to improve the seismic behavior of steel frames with CBF braces equipped with Shape Memory Alloy (SMA) and Buckling Restrained Braces (BRBs). In this manner, a multi-story building with inverted V chevron bracing was considered. Nonlinear time-history analyses have been performed using OpenSEES

software. The dynamic responses of frames with SMA and BRB braces were compared. The results showed that the SMA and BRB braces provide energy dissipation in the nonlinear zone and can reduce maximum interstory drift. The comparison of those bracing systems revealed that implementing SMA in braces also led to a reduction in permanent displacement of the structures due to the elasticity property of the SMA bracing system. The energy dissipation of structures with the BRB system was higher than that of structures with the SMA bracing system.

Keywords: buckling restrained brace, shape memory alloy, nonlinear analysis, time-history analysis, interstory displacement

Introduction

The design methodology of earthquake-resistant buildings has undergone many changes in recent years. Although these methods resulted in improved behavior of structures in past years, typical structural systems end up with high demand or internal forces in structural elements resulting from ground motion for high-rise structures. The collapse of many structures designed by conventional methods, the capability of employing robust analytical models, and significant improvement in computer performance are considerable factors in changing the design philosophy of structures during the preceding decade.[1] Recently, it has been shown that designing structures with fully elastic behavior in intense earthquakes is not an economical approach. As a result, such methods as the passive control of structures against earthquakes are used in their design; hence, the forces applied to the members of the structures are decreased to keep them from significant damage. In this context, structural control methods are categorized into active, passive and semi-active control (hybrid control). Passive control methods are generally categorized into two groups: energy dissipater and base isolation systems. All energy dissipaters that are used today have problems such as short useful lifetimes, fatigue, installation problems and the need for replacement after an earthquake and modification of the geometry of the structure after an earthquake.[2] Shape Memory Alloys (SMAs) are one type of smart material without many of these issues or limitations. They have been recently used for the passive control of structures as well as Buckling Restrained Braces (BRBs), which can dissipate energy extensively.[3] BRBs are used to try to improve the

seismic behavior of Concentric Braced Frames (CBFs) and also chevron braced frames, both of which exhibited a wide range of damage in the 1994 Northridge earthquake.[4] In this system, a bracing member is placed in a sleeve, which prevents buckling of the member. Therefore, the behavior of braces in compression is identical to that in tension (without buckling), which provides better ductility and energy dissipation compared with conventional bracing systems. It is worthwhile mentioning that passive control systems are often employed to retrofit existing structures with respect to new passive control systems.[5] For instance, Reference [6] has developed dissipative steel exoskeletons for reinforced concrete structures to improve the seismic performance of these structures and   reduce the seismic demand during an earthquake. In addition, hysteretically damped braces have shown enhanced seismic behavior even in asymmetric structures.[7]

The seismic behavior of steel structures with BRBs has been the focus of experimental studies in the past, and it has become the subject of analytic studies in recent years. Wakabayashi studied a reinforced concrete panel segregated by a steel layer. The experiment showed that the segregation process on the surface of the brace was significant in a panel bracing system. The bracing has resistance only to lateral force; however, a reinforced concrete panel only prevented the buckling of bracing.[8] Fundamental work on determining the response modification factor of BRB frames by Reference [9] has demonstrated that the BRB frames have high response modification factors; therefore, ductile performance is expected during strong ground shaking. Pushover studies and nonlinear dynamic analyses were performed to evaluate BRBs proposed for the seismic rehabilitation of four-story steel frames and unreinforced masonry walls damaged in the Kobe earthquake. The results of the test showed that the hysteresis behavior was stable and symmetric, and the seismic response was good. Three- and six-story buildings with BRBs under the influence of ground motions at different seismicity levels were analyzed in Reference [10]. In this research, the response modification factor of the BRBs was stated to be within the range 6–8, and it was suggested to use the BRB system for high-rise structures (9- to 20-story structures).[10] It was shown that an X-bracing system increased the stiffness of structures by studying concrete structures with BRBs; additionally, BRB systems not only improved stiffness but also provided the structure with appropriate ductility as well.[11] They

also showed that, as displacement exceeded the target zone and reached the safety zone, members had good seismic behavior. Additionally, their studies on the over-strength of these systems showed that BRBs had a high over-strength, which resulted in better performance of these systems in the nonlinear zone.[11]

Another structural seismic control system deploys SMAs, known as smart materials, which have advantages and unique properties compared with conventional energy dissipater systems. These include: they do not need to be replaced after an earthquake; they have high resistance to corrosion and fatigue; they remain elastic after being exposed to heat, they dissipate energy to a high degree, and they tolerate strain up to about 10% without leaving permanent strain. Furthermore, based on experimental and numerical studies of the application of SMAs on dampers and isolators, it was shown that using shape memory alloy improved the performance of bridges and buildings under earthquake loading.[13] SMAs are mounted in steel bracing in the form of wires, and their physical and geometrical properties include a module of elasticity, section area, and lengths of wires are chosen to idealize the expected behavior of bracing. Moreover, the steel section of braces is chosen so that only nonlinear deformation occurs, and energy dissipation only occurs in the damper zone, in order that the steel zone does not undergo plastic deformation.

In recent years, these alloys have been used to improve the performance level of structures in earthquakes. The use of seismic SMA-made dampers was studied thoroughly by Reference [16]. They examined the effect of frequency and loading history on the energy absorption of SMA-made cables. Additionally, they provided a one-dimensional model for modeling the semi-elastic behavior of such materials.[16] Reference [17] carried out experimental tests on a four-story building with an SMA bracing system using a shaking table. They concluded that the structural behavior is significantly improved by setting up the level of the initial tension of dampers to the natural frequency of the structure. It was also revealed that SMA-made cables might markedly reduce the deformation and acceleration of the structural response.[18] In Japan, a small-scale test was performed on a model bridge and it was concluded that SMA had better behavior in the martensite phase than in the austenite (super-elastic) phase.[19] Further, there is a series of papers entitled "MANSIDE" that consists of the most comprehensive studies of the SMA

bracing system on structures under dynamic loads. Reference [20] investigated diverse samples of various dimension under different loadings and measured their energy absorption and permanent strain under semi-static and dynamic loads at various frequencies. They concluded the following: (1) low or high loading frequency affects the behavior of SMAs; (2) as the number of loading cycles increases, energy dissipation decreases, and stiffness increases; (3) the damping of SMAs is low in the austenite phase, which helps the structure return to its original state; and (4) to obtain stable behavior of SMAs, they must be exposed to several loading cycles.[20] Furthermore, the analyses compare structures with traditional materials to structures with SMA materials as the retrofitting schemes in bracing systems. The results demonstrated that the SMAs acted like dampers, dissipated energy and lowered the imposed demand from seismic loads.[21]

One of the research efforts on employing SMAs in structures consisted of two laboratory studies on steel connections.[22] The authors tested beam-to-column connections made by SMAs and concluded that these connections had a stable hysteresis curve.[22] More recent studies of the use of SMAs in steel connections[23,24] showed acceptable interstory drifts as well as the control of residual deformations using SMA fuse bolts. A self-centering buckling- restrained brace was modeled (SC-BRB) by Ref. [25] that could dissipate energy as well self-center. This mechanism has a configuration that includes tubes compressed by floating anchorage plates connected to pre-tensioned superelastic NiTi shape memory alloy rods. They investigated the cyclic behavior and performance of a self-centering buckling-restrained brace as an experimental solution that provided an energy dissipation capability owing to having a typical BRB component that enabled additional energy dissipation. They concluded that the overall self-centering BRB behavior was robust and showed that, by fracture of the BRB core, the brace could still carry the load to a significant degree.[25] It was shown that decreasing the permanent deformation of a structure can cause the structure to undergo very small damage, and utilizing SMA in steel connections helps to reach this pivotal goal.[26] As the use of SMAs is increasing in various structures, new research has focused on applying SMA-based damping devices in a cable-stayed bridge and evaluating their function regarding temperature changes.[27] The response of a bridge under earthquake excitation was markedly reduced.[28]

In the present research, the seismic behavior of two types of bracing system, BRB and SMA, is studied and compared. Nonlinear static analysis is employed to investigate the seismic performance and ductility of the structure regarding the ultimate load and corresponding deflection capability of the structures. In addition, this study aims to bring up comprehensive comparative analyses between two proposed bracing systems in terms of the residual permanent displacement and interstory drift for structures with both BRB and SMA through nonlinear time-history analysis.

Design Methodology

Designing a Prototype Building— Properties and Assumptions

As shown in **Fig. 1,** the building considered in this research was 15 m in both length and width. The length of all spans was assumed to be 5 m. The bracing system was placed in the middle span in both directions. The stories were 3 m high. The axis-to-axis distance between columns was also 5 m. Three different structures in terms of height were modeled: 4-, 8- and 14-story structures so as to cover both low-rise and tall buildings. Braces were located in the middle span from the first story to the last story in the form of chevrons. For gravitational loading, the Iranian National Building Code–Part 6 was used,[29] which is based mostly

(A)   (B)
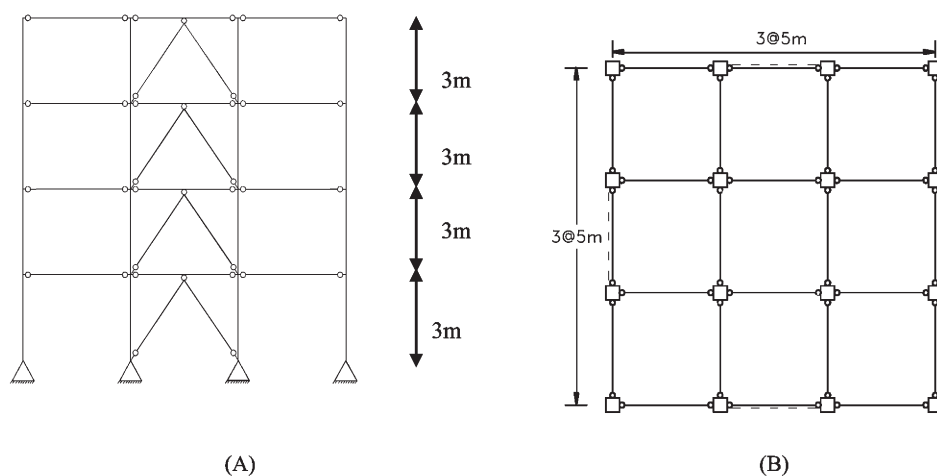
Fig. 1 Configuration of model structures: (A) side view; (B) brace location

on ASCE 7.[30] The dead load due to the ceiling and interior partition was 600 kg/m² for the stories and roof. The type of building was taken as residential; therefore, the live load was considered as 200 kg/m². Lateral loading was based on the 2800-V3 Iranian Code,[31] which mainly follows the seismic loading section of ASCE 7.[30] The structural analysis methodology used in this article for lateral and seismic loads was the equivalent static method.

The site location considered for the design was Tehran, Iran, and most parts of this city have soil of the Type II soil category. The importance factor was taken to be one, owing to the type of building (residential). Also, the response modification factor of the structure was considered to be six, based on the 2800-V3 Iranian Code.[31] The analytical periods of the first mode were 0.31, 0.51 and 1.02 s for 4-, 8- and 14- story structures, respectively. The steel design of the building used the Load and Resistance Factor Design (LRFD) approach based on Iranian National Building Code–Part 10,[32] which is based on AISC 2016[33] and modeled by SAP2000® software.[34] **Tables 1–3** show the outcome of designing the sections for these structures under gravitational and lateral (seismic) loads.

Table 1 Sections in a four-story building (modeled frame)—unit for column sections, millimeters

Column in D1 axis	Column in D2 axis	Column in D3 axis	Column in D4 axis	BRB cross section, A_{eq} (cm²)
Box 100×100×8	Box 160×160×16	Box 160×160×16	Box 100×100×8	44
Box 100×100×8	Box 160×160×10	Box 160×160×10	Box 100×100×8	44
Box 100×100×8	Box 100×100×10	Box 100×100×10	Box 100×100×8	35.84
Box 100×100×8	Box 100×100×8	Box 100×100×8	Box 100×100×8	35.84

Table 2 Sections in an eight-story building (modeled frame)—unit for column sections, millimeters

Story	Column in D1 axis	Column in D2 axis	Column in D3 axis	Column in D4 axis	BRB cross section, A_{eq} (cm²)
1st	Box 120×120×10	Box 300×300×35	Box 300×300×35	Box 120×120×10	112
2nd	Box 120×120×10	Box 300×300×35	Box 300×300×35	Box 120×120×10	112
3rd	Box 100×100×10	Box 240×240×28	Box 240×240×28	Box 100×100×10	112
4th	Box 100×100×8	Box 240×240×28	Box 240×240×28	Box 100×100×8	79.36
5th	Box 100×100×8	Box 180×180×16	Box 180×180×16	Box 100×100×8	79.36
6th	Box 100×100×8	Box 180×180×16	Box 180×180×16	Box 100×100×8	79.36
7th	Box 100×100×8	Box 120×120×10	Box 120×120×10	Box 100×100×8	52

Table 3 Sections in a 14-story building (modeled frame)—unit for column sections, millimeters

Story	Column in D1 axis	Column in D2 axis	Column in D3 axis	Column in D4 axis	BRB cross section, A_{eq} (cm²)
1st	Box 120×120×20	Box 500×500×50	Box 500×500×50	Box 120×120×20	128
2nd	Box 120×120×20	Box 500×500×50	Box 500×500×50	Box 120×120×20	128
3rd	Box 120×120×16	Box 450×450×40	Box 450×450×40	Box 120×120×16	128
4th	Box 120×120×16	Box 450×450×40	Box 450×450×40	Box 120×120×16	128
5th	Box 120×120×16	Box 400×400×30	Box 400×400×30	Box 120×120×16	112
6th	Box 120×120×16	Box 400×400×30	Box 400×400×30	Box 120×120×16	112
7th	Box 120×120×16	Box 340×340×25	Box 340×340×25	Box 120×120×16	112
8th	Box 100×100×10	Box 340×340×25	Box 340×340×25	Box 100×100×10	96
9th	Box 100×100×10	Box 300×300×16	Box 300×300×16	Box 100×100×10	96
10th	Box 100×100×10	Box 300×300×16	Box 300×300×16	Box 100×100×10	96
11th	Box 100×100×10	Box 160×160×20	Box 160×160×20	Box 100×100×10	66.56
12th	Box 100×100×10	Box 120×120×20	Box 120×120×20	Box 100×100×10	66.56
13th	Box 100×100×10	Box 120×120×20	Box 120×120×20	Box 100×100×10	44
14th	Box 100×100×10	Box 100×100×10	Box 100×100×10	Box 100×100×10	36

BRB Design and Specifications

These braces have a ductile steel core that reaches the yield limit under both strain and compressive stress. The core is placed inside a hollow steel casting to prevent buckling under pressure, and then the cast is filled with mortar or concrete. To design the BRB members, the internal axial forces for each brace were determined as the output from analyzing the structures. The BRB components included parts such as a yielding core, an unrestrained non-yielding segment and a transition zone (see **Fig. 2**). In this study, the BRB design methodology proposed
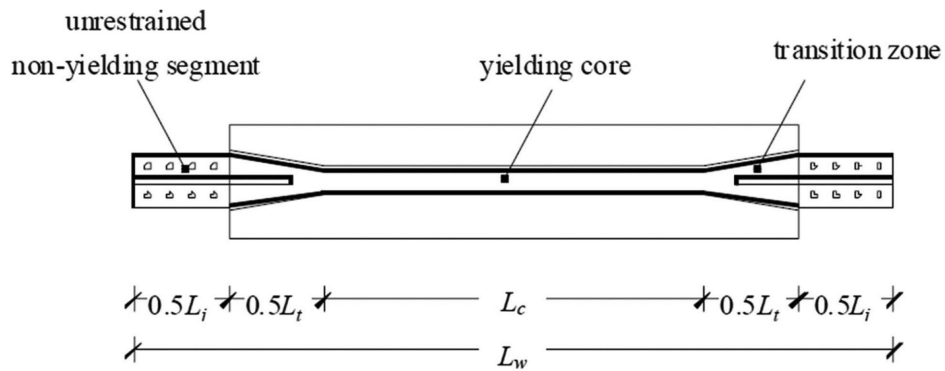
Fig. 2 Schematic of a BRB12

by Reference [12] was used to obtain the cross-sectional areas of these elements. The equivalent cross-sectional area A_{eq} should be computed, and is given by the following equation:

$$A_{eq,i} = \frac{A_{c,i}}{\frac{L_j}{L_w}\frac{A_c}{A_j} + \frac{L_t}{L_w}\frac{A_c}{A_t} + \frac{L_c}{L_w}}$$ (1)

$$A_{c,i} = \frac{V_{Ed,i}}{2f_y\cos\theta}$$ (2)

where L_c is the length of the yielding core, $0.5L_t$ is the length of the transition zone, $0.5L_j$ is the length of the unrestrained non-yielding segment and L_w is the length of the whole brace. In addition, $A_{c,i}$ is the cross-sectional area of the yielding core of the ith story (where i refers to the number of the story) and can be calculated using Eq. (2), A_j is the unrestrained non-yielding segment and A_t is the transition zone. The last columns in Tables 1–3 indicate the cross-sectional areas for BRB members in each story. As expected, the cross-sectional area of the BRBs is lower in higher stories due to less demanding internal forces.

Shape Memory Alloy Design

To compare the seismic performance of SMAs and BRBs, SMA braces were designed to have the same yield strength, F_y, and the identical axial stiffness, K, as BRBs. For this reason, the structures with SMA-type bracing had the same natural frequency as the structures employing the BRB system. Both the steel elements and the SMA elements had the same yield force. To this end, the following stages were proposed by Reference [15]:

$$A^{SMA} = \frac{F_y}{\sigma_s^{AS}} = \frac{2400 \times A^{Steel}}{4140}$$
$$= 0.58 \times A^{Steel}$$ (3)

$$L^{SMA} = \frac{E^{SMA} \times A^{SMA}}{0.08 \times L^{Steel}}$$
$$= \frac{275790 \times 0.58 A^{Steel}}{2e6 \times A^{Steel} \times L^{Steel}}$$
$$= 0.08 \times L^{Steel}$$ (4)

where A^{SMA} denotes the equivalent cross-sectional area of SMA bracing, A^{Steel} is the equivalent cross-sectional area of BRB bracing, L^{Steel} is the length of the BRB, L^{SMA} is the length of an SMA brace and σ_s^{AS} is the stress of phase conversion from austenite to martensite.

Therefore, the length of the SMA part is 0.08 of the brace length, and the cross section of the SMA part is 0.58 of the equivalent brace cross-sectional area. **Table 4** shows the mechanical properties considered for SMA material in calculations and numerical simulation.

Table 4 Mechanical properties considered for memory material

Quantity	Value (MPa)
Steel elasticity module (E_{Steel})	200,000
SMA elasticity module (E_{SMA})	27,579
Stress at start of austenite-to-martensite phase conversion (σ^{AS}_S)	414
Stress at the end of austenite-to-martensite phase conversion (σ^{AS}_F)	550
Stress at start of martensite-to-austenite phase conversion (σ^{SA}_S)	390
Stress at the end of martensite-to-austenite phase conversion (σ^{SA}_F)	200
Equivalent strain of length of stress smoothening (ε_L)	3.5%

Numerical Modeling for Nonlinear Analyses

To carry out the nonlinear analyses, the prototype building was modeled in OpenSEES.[14] This software has a full archive of various linear and nonlinear behaviors, including the definition of materials, steel or concrete elements, and the definition of varied elements for modeling. Besides the elements that are available in the archive, users can arbitrarily determine some materials and elements for their modeling. In this section, the types of element and also the material properties utilized in component modeling in OpenSEES are explained. In this context, to model the beams and columns, nonlinear beam–column elements with fiber sections were used. The inelastic material properties were selected in accordance with Steel02 as shown in **Fig. 3**a. The P–Δ effects were considered, and 5% was assigned for the damping ratio. All beam–column connections were pinned joints. For considering the buckling of columns,
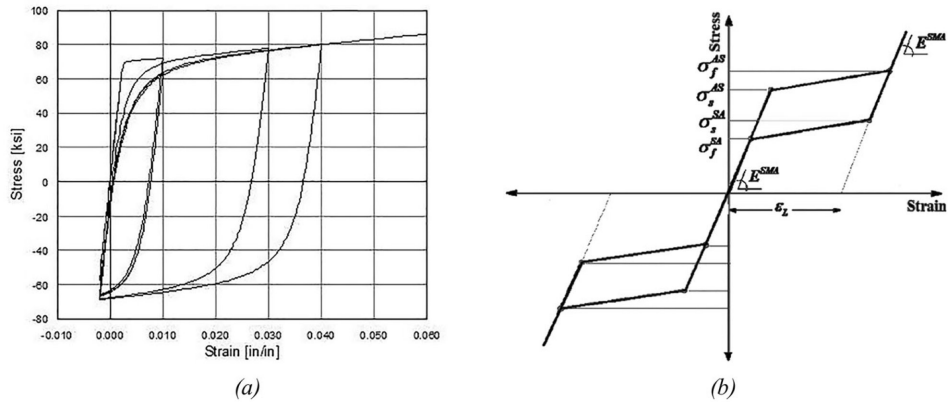
Fig. 3 Behavioral model of materials: (a) beam, column and BRBs (Steel02);14 (b) superelastic bracing (SMA)[15]

the primary angular rotation was taken as 0.01% of the column length (equal to 0.3 mm herein).

Meanwhile, the braces in the companion with SMA parts were modeled using the same element type as the beams and columns, and the material properties were selected similar to those of the beams and columns as well. Furthermore, the strain-hardening slope was 2%. The SMA bracing system included both rigid and memory alloy parts. Since the length of the SMA members in a brace was shorter than the overall length of the brace, the rigid part was used. By doing so, the overall deformation in a brace resulting from the deformation of the memory members was guaranteed. In this research, the SMA members were assumed to be a combination of several super elastic rods that tolerate a compression load without undergoing buckling.

For purpose of verifying the materials used, the response of the numerical analysis was compared with the experimental results given in two articles from the literature. **Figure 4** shows a stress–strain comparison between the numerical analysis and experimental results from the literature. Further information can be gleaned by referring to the literature.[35,36]

Since the beam–column connections were pinned joints, this has been considered in the modeling of frames. To this end, separate nodes were defined at the ends of all beams and columns. Then, the two nodes with the same coordinates were connected and constrained only at the transition degrees of freedom using the equalDOF command. Moreover,
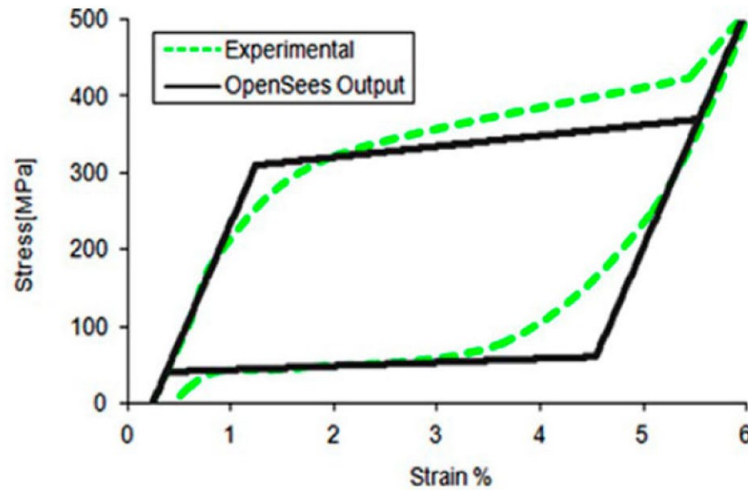
Fig. 4 Stress–strain diagram of OpenSEES and experimental results

column bases were pinned joints, and the floors of stories were considered in a rigid form. The mass of the stories was defined as a lumped mass at one point. Figure 2b shows the SMA model parameters used in modeling schematically.

Lumped plasticity was used for modeling plastic deformations in the system, and the stiffness-based Rayleigh model was used for damping in the structure, following the recommendations of Reference [37]. In this model, columns and beams have an elastic element in the middle of them, and the ends include two nonlinear rotational springs. The behavior of the backbone curve for this moment is based on a modification of that used by Ibarra and Krawinkler.[38]

Numerical Results

In this section, the results of nonlinear static and time-history dynamic analyses are investigated. Analyses are performed for different static and dynamic analyses in linear and nonlinear states. These analyses provide an estimation of the lateral capacity of structures or available engineering demand parameters (e.g. interstory drift) during ground motion records applied to the structures.

Nonlinear Static Analysis Study

All structures under constant gravitational and increasing lateral load with inverse triangular load patterns were subjected to a displacement slightly more than their target displacement, and nonlinear static analysis was carried out. It was assumed that the fundamental mode of vibration of the structure was the dominant model in an earthquake; therefore, the definition of the inverse triangular loading pattern was based on this assumption. **Figure 5** presents capacity curves obtained from nonlinear static analyses of 4-, 8- and 14-story structures having BRBF and SMAF bracing.

From Fig. 5c, it is observed that, as the number of stories increases, the primary stiffness of the structure decreases. Furthermore, the primary and ultimate yield strength of the structure increases. By comparing them with SMA and BRB braces, it can be concluded that energy dissipation, strain hardening, and primary and ultimate strength of structures with BRB are higher compared with structures using an SMA bracing system. Additionally, it seems that the energy dissipation
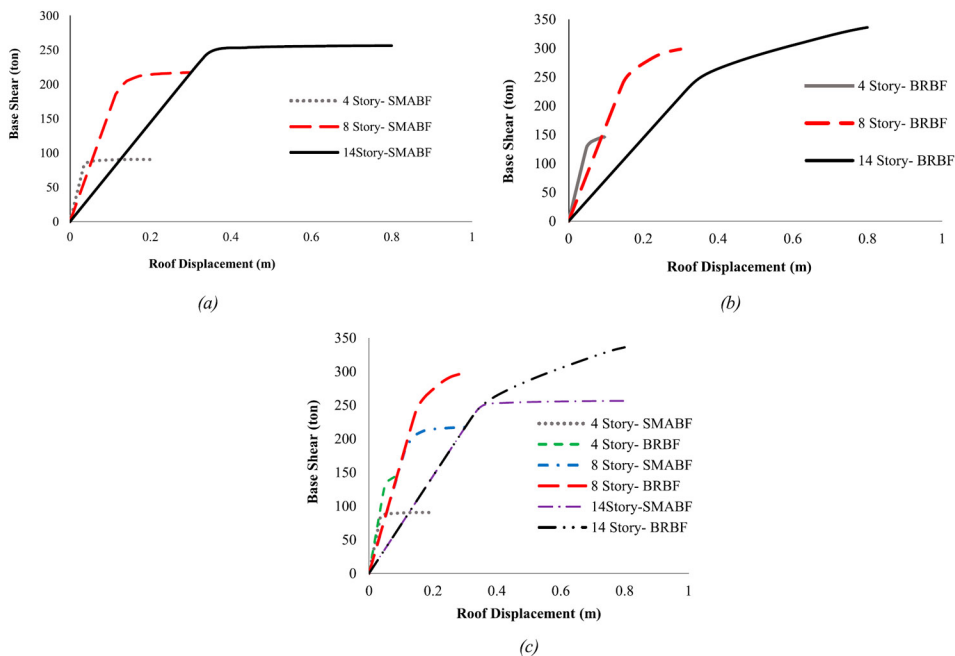
Fig. 5 Diagram of base shear–roof displacement of the highest story: (a) structures with SMABF bracing; (b) structures with BRBF bracing; (c) structures with SMABF and BRBF bracing

capability of a four-story structure with SMA bracing is higher compared with that of a BRB bracing structure. Thus, due to the relatively high strain hardening of structures with BRB bracing and the low ductility of BRB bracing, the energy produced by the earthquake is not dissipated by the building. Consequently, large forces are applied to the columns, which make the columns undergo buckling and leads to the collapse of the structure. However, as the number of stories increases, this problem is reduced in structures with BRB bracing.

It is worthwhile mentioning that the elasticity property of SMA bracing, the capability of replacement, and their low permanent displacement should not be neglected. In the following, the seismic behavior of these structures under nonlinear dynamic analysis is evaluated.

Nonlinear Time-history Analysis

Owing to differences in the intensity, duration and frequency content of various earthquakes, their effects differ in the dynamic response of structures. Additionally, the frequency content has a more substantial effect; therefore, if the dominant earthquake frequency matches the natural frequency of the structure, it will cause the highest damaging effect. Hence, earthquake or ground motion records must be chosen such that they cover a wide range of frequencies.

Moreover, according to 2800 Iranian earthquake standards,[31] at least three records must be used. Hence, three earthquakes with different frequency content and Type II soil (equal to 'D' category of ASCE 7–10 code[30]) were chosen in this research, as shown in **Table 5.**

Table 5 Ground motion data

Earthquake	Year	PGA (g)	Duration (s)
El Centro	1940	0.348	53.74
Kobe	1995	0.599	48
Tabas	1978	0.934	35

The scaling approach is based on the 2800 standard as follows.

- All records are scaled to their maximum acceleration. In other words, their maximum acceleration reached the gravity acceleration.
- The response spectrum of each record is obtained by considering 5% damping.
- The obtained response spectra are scaled between 0.2 and 1.5 T, where T is the fundamental period of the structure.
- The achieved scale factor should be multiplied by records that have been scaled in the first step and then used in dynamic analysis.

To present the results of nonlinear dynamic analysis, five parameters, i.e. the highest interstory displacement during the analysis, the axial force curve, the first story displacement, the story-displacement-to-story-height ratio, and the maximum permanent roof displacement of the structure, are considered.

Figures 6 and 7 display the time history and relative displacement of 4-, 8- and 14-story frames for nonlinear time-history analysis. The maximum roof displacement and the permanent displacements are evident in these figures. Although beam and column sections are identical for both the BRB system and SMA system, the behavior of BRB and SMA after passing the elastic level have significant differences.

As shown in **Fig. 8,** the maximum displacement is higher in all SMA-BFs compared with BRBFs. When structural bracing enters the nonlinear zone, the behavior of the two structures compared to each other demonstrates significant changes. In this manner, the SMAB system has less permanent displacement owing to its super-elastic behavior in comparison with a BRB system. However, SMAB systems have a higher frequency response and experience a higher maximum relative displacement during an earthquake as compared with BRB systems, which is explained by numerous changes in the stiffness and strength of bracing and multiline behavior of these materials subject to the seismic cyclic load.

Figures 9–11 illustrate the behavior of the first story for the BRB and SMA systems. As shown, the BRB system is able to dissipate energy more than the SMA system, but the SMA system has better behavior and control over the members in terms of plastic displacements because of its restoration behavior as well as dissipating energy.

(a)

(b)

(c)
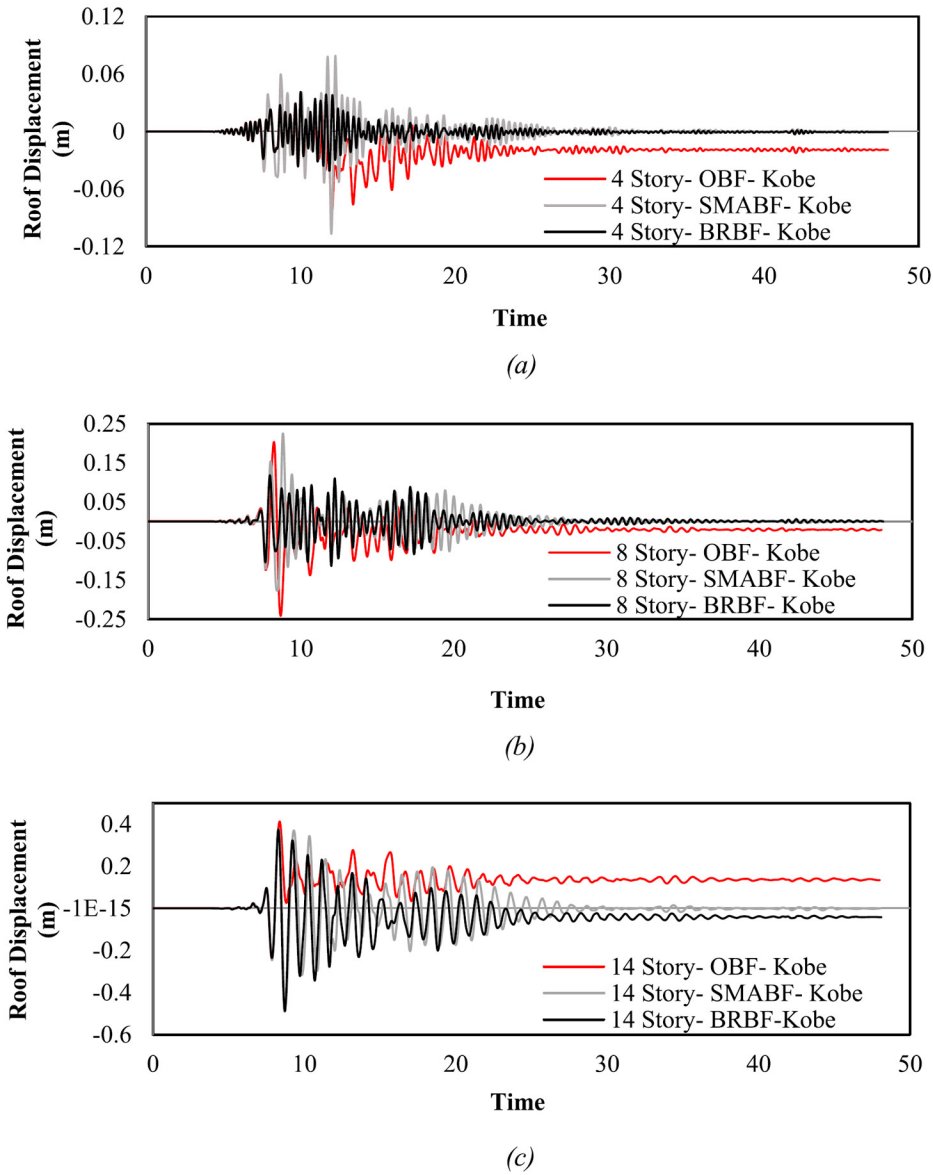
Fig. 6 Time history of roof displacement: (a) a four-story frame subjected to the Kobe earthquake; (b) an eight-story frame subjected to the Kobe earthquake; (c) a 14-story frame subjected to the Kobe earthquake
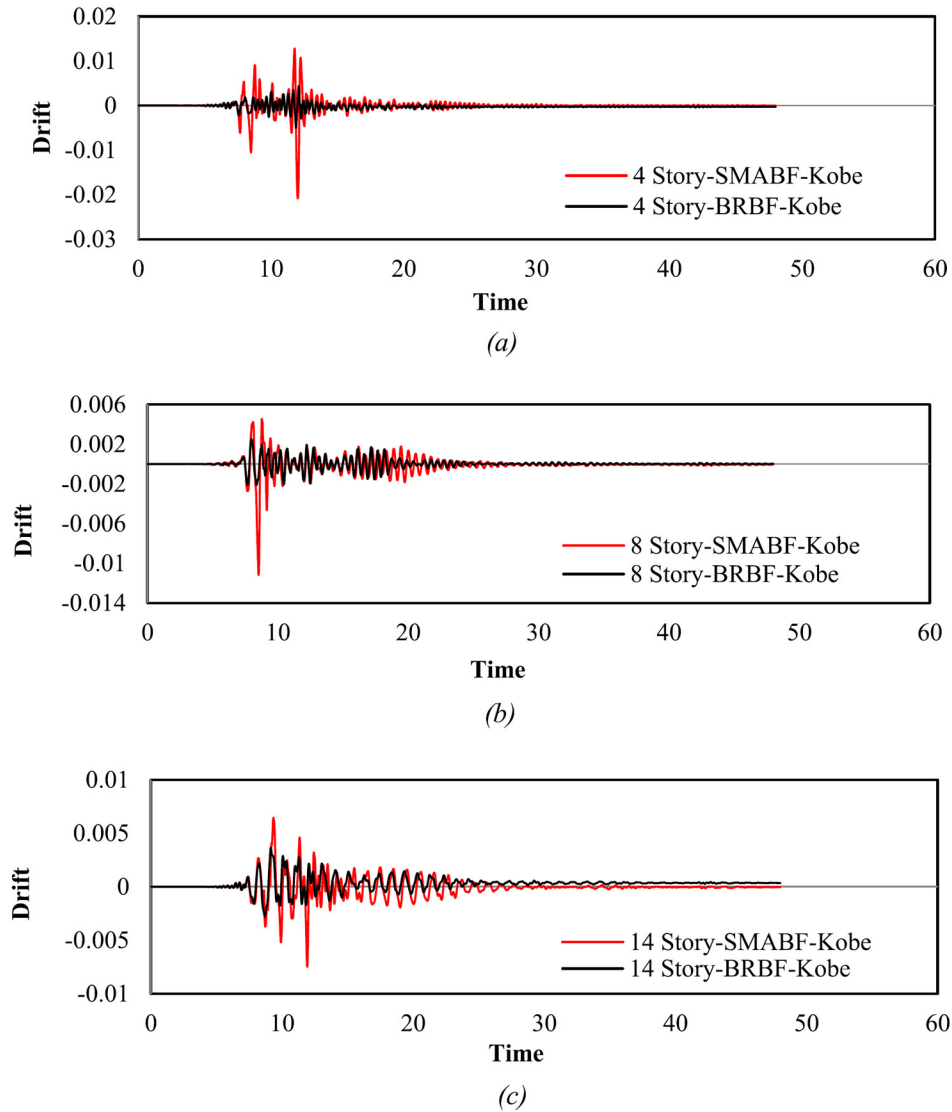
Fig. 7 Relative displacement history: (a) the first story of a four-story frame subjected to the Kobe earthquake; (b) the first story of an eight-story frame subjected to the Kobe earthquake; (c) the first story of a 14-story frame subjected to the Kobe earthquake

Elcentro Ground Motion

(a)

Kobe Ground Motion

(b)

Tabas Ground Motion

(c)
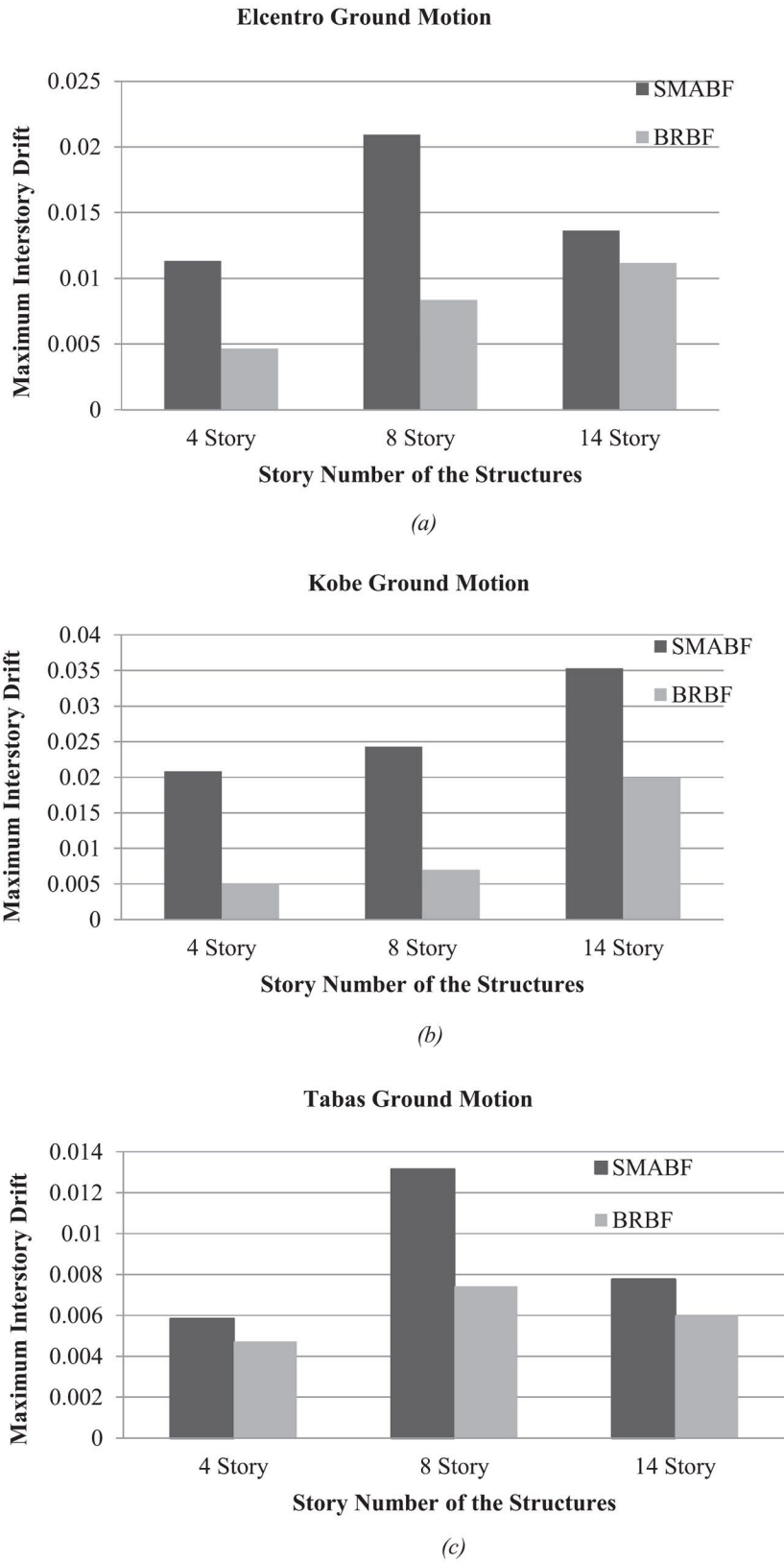
Fig. 8 The maximum relative interstory displacement: (a) the El Centro earthquake; (b) the Kobe earthquake; (c) the Tabas earthquake

(a)

(b)
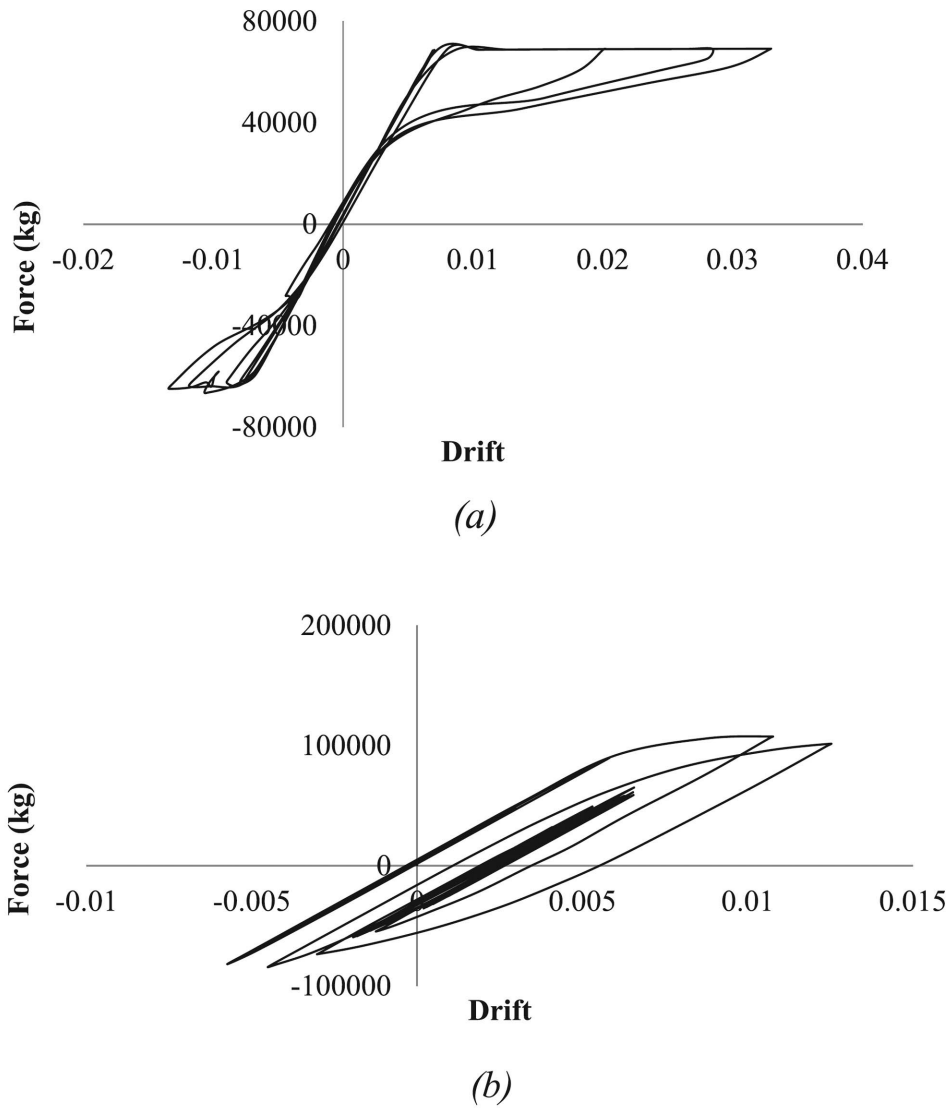
Fig. 9 Axial force–displacement curve of the first story of a four-story frame in the El Centro earthquake: (a) SMA; (b) BRB

(a)

(b)
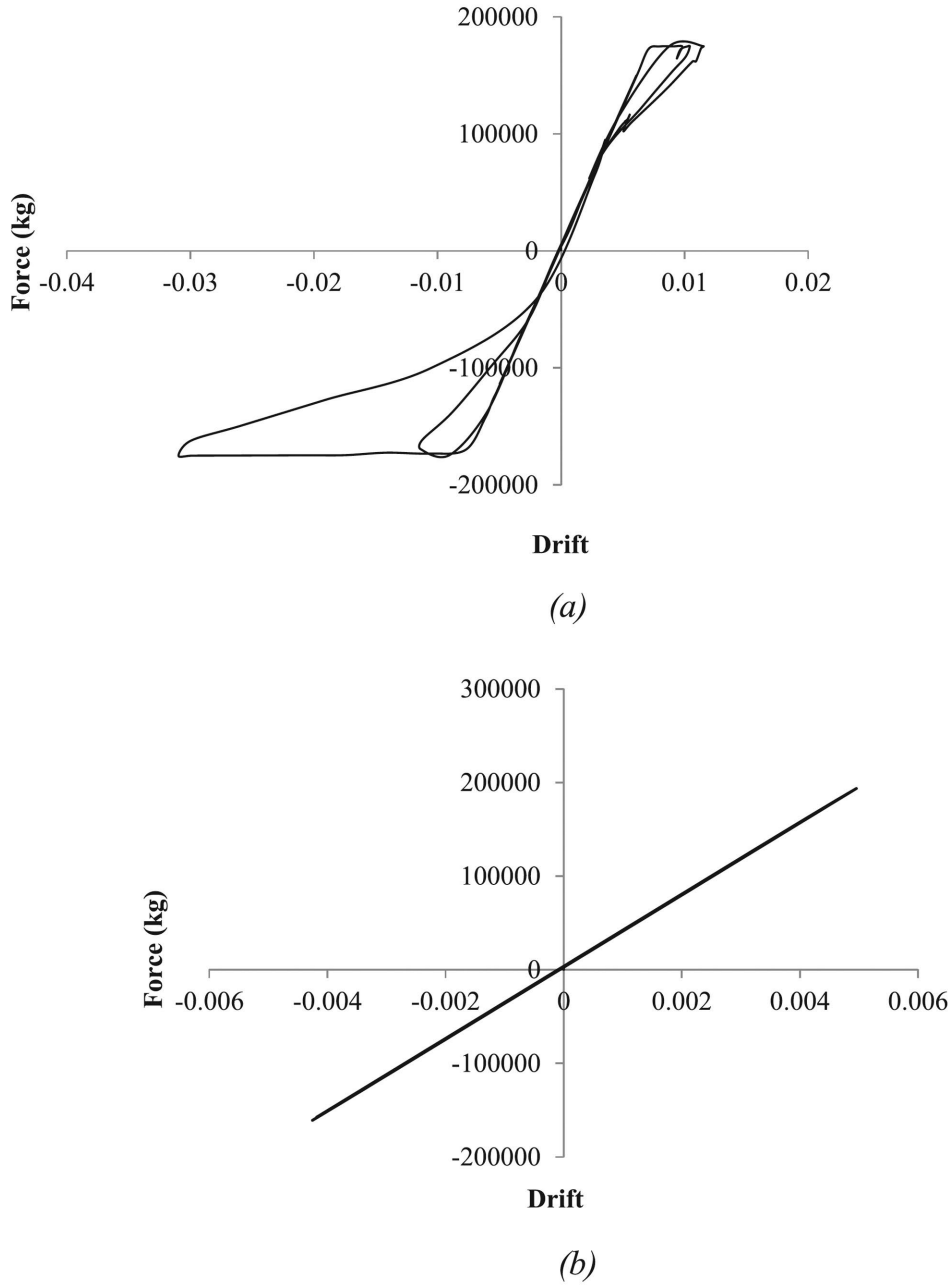
Fig. 10 Axial force–displacement curve of the first story of an eight-story frame in the Kobe earthquake: (a) SMA; (b) BRB

(a)

(b)
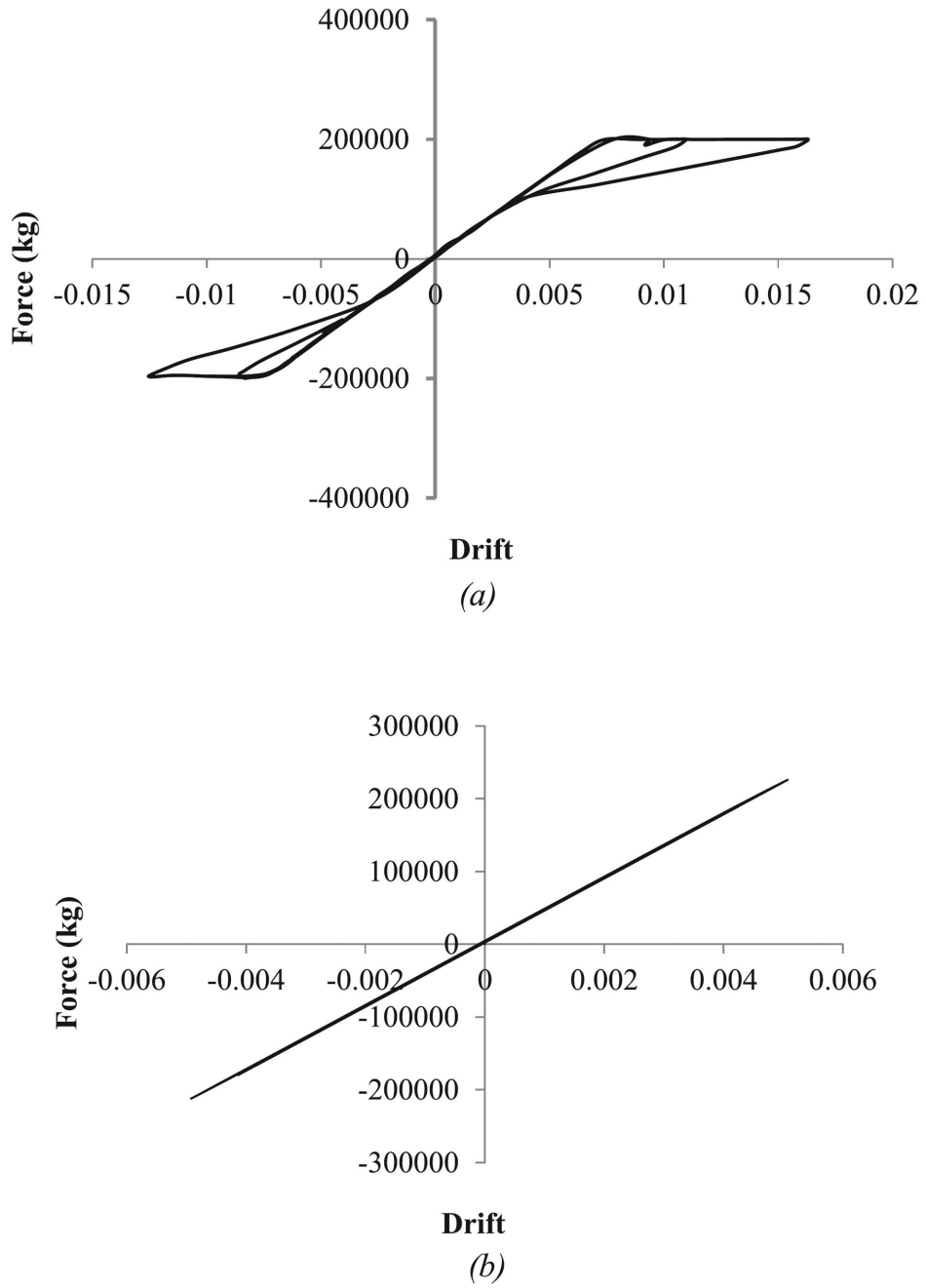
Fig. 11 Axial force–displacement curve of the first story of a 14-story frame in the Kobe earthquake: (a) SMA; (b) BRB

The axial force–displacement curve of the first story shows very much the general behavior of bracing systems. For structures with an SMA bracing system, the diagram is flag-shaped, and it is observed that deformation is higher in the SMA brace compared with the BRB brace. Furthermore, the SMA brace had fewer permanent deformations because of its elastic behavior. It is evident from diagrams related to BRB bracing that it maintains its primary slope and only experiences permanent strain after entering the nonlinear zone when the direction of loading changes. That is, it is high in intense earthquakes and causes the diagram to become fat, which indicates high seismic energy absorption. Moreover, in structures with more stories, it is evident that SMA braces enter the nonlinear zone earlier than BRB bracing; therefore, the force applied to the main structural elements is reduced, and a more ductile behavior is shown compared with BRBs in SMABFs.

Figure 12 depicts the maximum relative interstory displacement for SMA structures, which is higher than the corresponding values for BRB structures in most cases. Further, the reason behind the large differences between the relative displacement of a couple of models is related to the transferring of huge amount of force from brace to beam or column. This means that it is caused by the full conversion of the martensite phase (the re-stiffening stage: the stage following the smoothing of loading in a super-elastic diagram) and loss of elasticity by an SMA brace in this phase. Subsequently, big displacements and large relative displacements in the story occurred.

Referring to **Fig. 13** in relation to permanent displacement of the roof of the highest story in different structures, the role of an SMA bracing system in reducing permanent displacement becomes clearer. The main feature of an SMA bracing system is its unique elasticity property. These results show the benefit of SMA-based bracing systems over other systems, even over BRBs. By implementing SMA in bracing systems to reduce or approximately exclude permanent displacement, it must be ensured that re-stiffening of these materials results in transferring a large force to other structural members. Transferring large forces from brace to beam or column, owing to full conversion of the martensite phase, results in the transfer of yield force to other structural members. In such cases, one can reduce the stress level of the phase conversion limit by changing the length and cross-sectional area of the SMAs. As a result, no permanent displacement occurs in the structure.

(a)

(b)

(c)
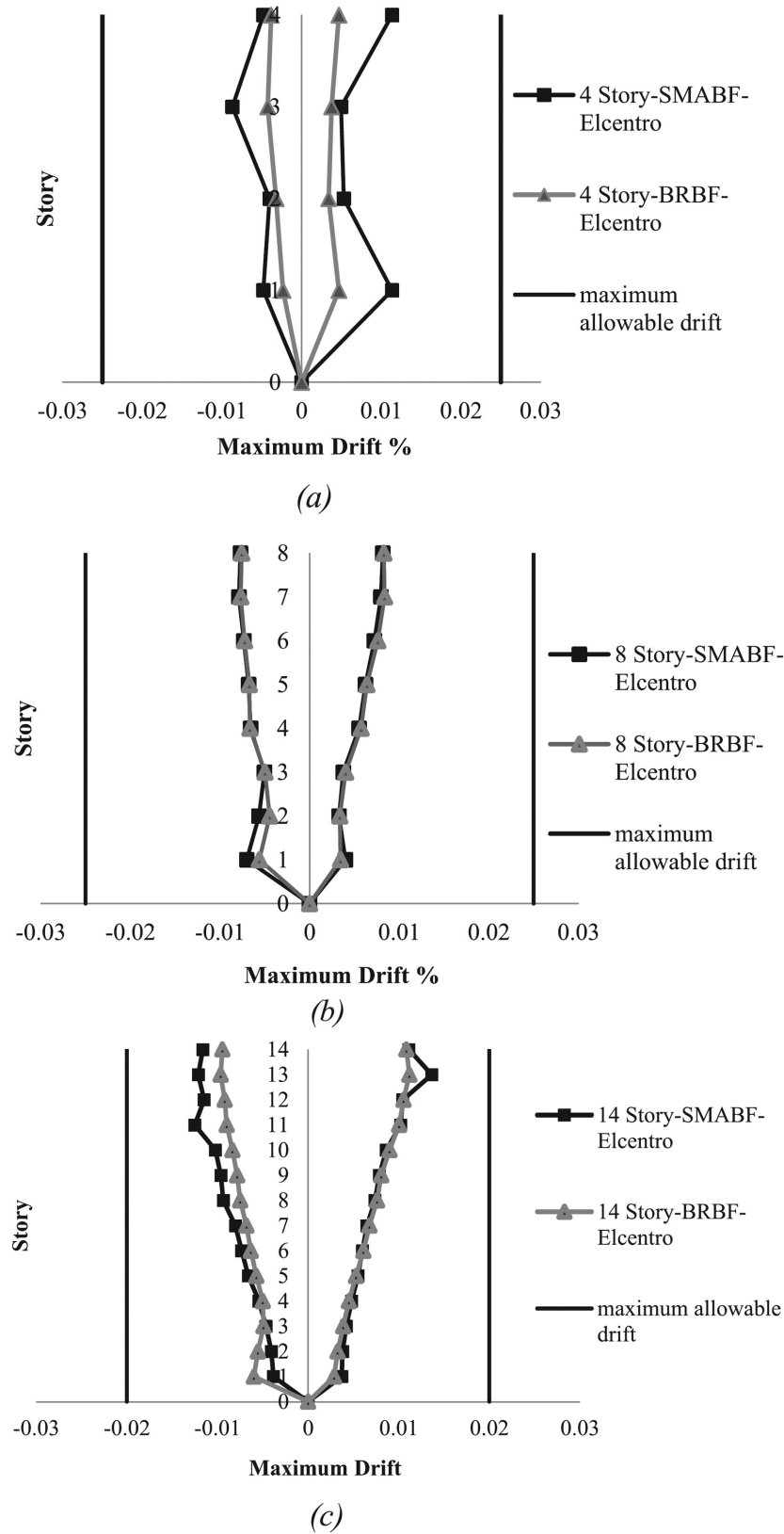
Fig. 12 Story-displacement-to-story-height ratio when subjected to the El Centro earth-quake: (a) four-story building; (b) eight-story building; (c) 14-story building

(a)

(b)

(c)
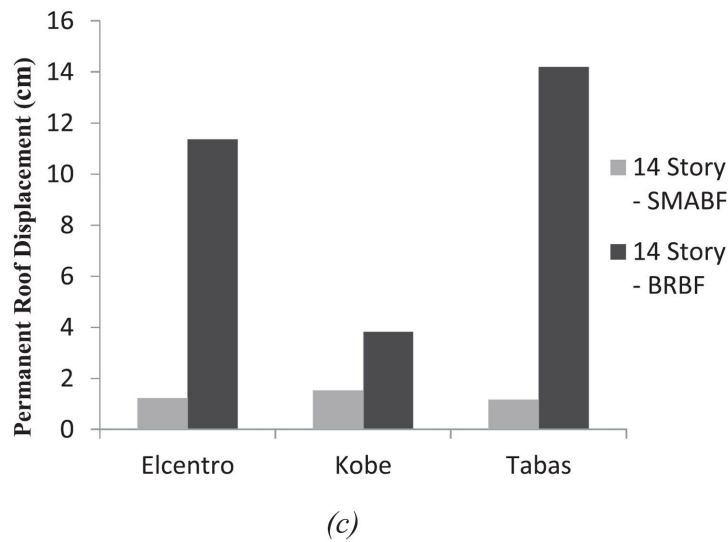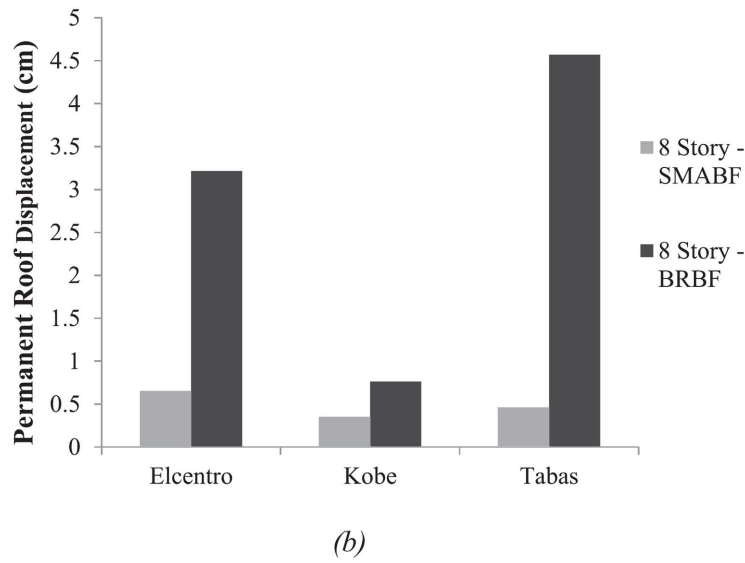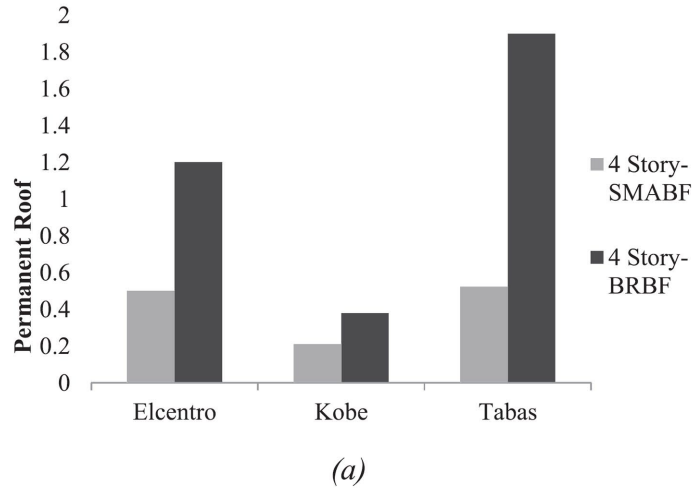
Fig. 13 Permanent roof displacement when subjected to the El Centro, Kobe and Tabas earthquakes: (a) four-story frame; (b) eight-story frame; (c) 14-story frame

Conclusions

It can be concluded from the nonlinear static analysis of frames that, as the number of stories increases, the initial stiffness of the structure decreases. In addition, the initial and ultimate yield strength of the structure increases. The comparison of SMA bracing structures with BRB bracing revealed the energy dissipation and primary and ultimate yield strength of structures with BRB higher than those of SMA bracing structures. Given the maximum values of relative interstory displacement, it is observed that SMABF drift values are higher than those of BRBs. Moreover, owing to the high ductility of these materials, one must be careful about structural drift, which should not exceed allowable drift.

The axial force–displacement curve for the first story shows very much the general behavior of a bracing system. For structures with SMA bracing systems, the diagram is flag-shaped. The SMA braces also have much less permanent strain owing to their elastic behavior. Additionally, both systems have more stable hysteresis curves compared with the hysteresis curves of conventional bracing systems. Diagrams of the maximum relative displacement of stories with respect to story height show the structure's response for different stories of the structure. In most cases, the maximum relative interstory displacement is higher for structures with SMA bracing compared with corresponding values for structures with BRB bracing.

Comparison of the permanent roof displacement for the frames is another important study conducted in this research. From results of the roof displacement time history of the highest stories of structures with different stories and bracing systems, the role of SMA braces in the reduction of vibration of the structure becomes evident. In most cases, the comparison between different bracing systems shows that the use of SMA bracing results in the reduction of permanent displacement in the structure due to the unique elasticity property of SMA bracing systems.

It is not recommended to use SMA bracing systems in a location where the likelihood of high-intensity earthquakes is low because these materials are expensive. In addition, their behavior in weak earthquakes is very similar to that of BRBs, and the use of BRBs is preferred in these conditions. In places where there is a high likelihood of intense earthquakes, the use of SMABF has priority over using BRBF because almost

the whole seismic energy is dissipated in the first mode of vibration. Owing to the high ductility of structures with an SMA bracing system, the drift of stories may exceed the permissible drift, which must be considered in the design of the structure.

* * * * *

Disclosure No potential conflict of interest was reported by the authors.

Data Availability The raw/processed data required to reproduce these findings cannot be shared at this time as the data also forms part of an ongoing study.

References

[1] Soraghi A, Huang Q. Probabilistic prediction model for RC bond failure mode. Eng Struct. 2021; 233: 111944. https://doi.org/10.1016/j.engstruct.2021.111944

[2] Abasi A, Harsij V, Soraghi A. Damage detection of 3D structures using nearest neighbor search method. Earthq Eng Eng Vib. Jul. 2021; 20(3): 705–725. https://doi.org/10.1007/s11803-021-2048-1

[3] Motahari S, Ghassemieh M, Abolmaali S. Implementation of shape memory alloy dampers for passive control of structures subjected to seismic excitations. J Constr Steel Res. 2007; 63(12): 1570–1579.

[4] Rai DC, Goel SC. Seismic evaluation and upgrading of chevron braced frames. J Constr Steel Res. 2003; 59(8): 971–994.

[5] Benavent-Climent A. An energy-based method for seismic retrofit of existing frames using hysteretic dampers. Soil Dyn Earthq Eng. 2011; 31(10): 1385–1396.

[6] Mazza F. Dissipative steel exoskeletons for the seismic control of reinforced concrete framed buildings. Struct Control Heal Monit. Mar. 2021; 28(3). https://doi.org/10.1002/STC.2683

[7] Mazza F. Nonlinear seismic analysis of unsymmetric-plan structures retrofitted by hysteretic damped braces. Bull Earthq Eng. 2016; 14(4): 1311–1331.

[8] Wakabayashi M, et al. Experimental study of elasto-plastic properties of precast concrete wall panels with built-in insulating braces. Summ Tech Papers Annu Meet. 1973; 1: 041–1.

[9] Asgarian B, Shokrgozar HR. BRBF response modification factor. J Constr Steel Res. 2009; 65(2): 290–298.

[10] Sabelli R, Mahin S, Chang C. Seismic demands on steel braced frame buildings with buckling-restrained braces. Eng Struct. 2003; 25 (5): 655–666.

[11] Rahai A, Alinia M. Performance evaluation and strengthening of concrete structures with composite bracing members. Constr Build Mater. 2008; 22(10): 2100–2110.

[12] Barbagallo F, Bosco M, Marino E, Rossi P. Seismic performance and cost comparative analysis of steel braced frames designed in the framework of EC8. Eng Struct. 2021; 240: 112379.

[13] Alam M, Youssef M, Nehdi M. Utilizing shape memory alloys to enhance the performance and safety of civil infrastructure: a review. Can J Civ Eng. Sep. 2007; 34(9): 1075–1086. https://doi.org/10.1139/L07-038

[14] Fenves GL, Mazzoni FMS, Scott MH. Open system for earthquake engineering simulation OpenSees. Comput Sci Eng. 2004; 13(4): 58–66. https://doi.org/10.1109/MCSE.2011.66

[15] Asgarian B, Moradi S. Seismic response of steel braced frames with shape memory alloy braces. J Constr Steel Res. 2011; Volume: 67(1): 65–74.

[16] Graesser EJ, Cozzarelli FA. Shape-memory alloys as New materials for aseismic isolation. J Eng Mech. Nov. 1991; 117(11): 2590–2608. https://doi.org/10.1061/(ASCE)0733-9399(1991)117:11(2590)

[17] Inaudi J, Kelly JM. Experiments on tuned mass dampers using viscoelastic, frictional and shape-memory alloy materials. First World Conference on Structural Control. 1994: 127–136.

[18] Sweeney SC, Hayes J. Shape memory alloy dampers for seismic rehabilitation of existing buildings. Proceedings of 27th Joint Meeting on Wind and Seismic Effects. 1995: 317–332.

[19] Adachi Y, Unjoh S. Development of shape memory alloy damper for intelligent bridge systems. Smart Struct Mater. 1999; 3671: 31–42.

[20] Dolce M, Cardone D. Mechanical behaviour of shape memory alloys for seismic applications 2. Austenite NiTi wires subjected to tension. Int J Mech Sci. 2001; 43(11): 2657–267.

[21] Bruno S, Valente C. Comparative response analysis of conventional and innovative seismic protection strategies. Earthq Eng Struct Dyn. 2002; 31(5): 1067–1092. https://doi.org/10.1002/eqe.138

[22] Desroches R, Asce M, Mccormick J, Delemont M. Cyclic properties of superelastic shape memory alloy wires and bars. J Struct Eng. Jan. 2004; 130(1): 38–46. https://doi.org/10.1061/(ASCE)0733-9445(2004)130:1(38)

[23] Rad Z, Ghobadi M, Yakhchalian M. Probabilistic seismic collapse and residual drift assessment of smart buildings equipped with shape memory alloy connections. Eng Struct. 2019; 197: 109375.

[24] Farooghi-Mehr SM, Ghobadi MS. Cyclic behavior of reinforced welded flange plate moment connections with triangular stiffener plates. J Struct Constr Eng. 2019; 6(1): 5–23.

[25] Miller D, Fahnestock L, Eatherton M. Development and experimental validation of a nickel–titanium shape memory alloy self-centering buckling-restrained brace. Eng Struct. 2012; 40: 288–298.

[26] Sultana P, Youssef M. Seismic performance of steel moment resisting frames utilizing superelastic shape memory alloys. J Constr Steel. 2016; 125: 239–251.

[27] Zhang N, Chang R, Gu Q. Response sensitivity studies of a cable-stayed bridge with shape memory alloy damping system considering temperature effects. Eng Struct. 2021; 244: 112772.

[28] Soraghi A, Huang Q. Simple rebar anchorage slip macromodel considering corrosion. Eng Struct. Jul. 2022; 262: 114357. https://doi.org/10.1016/J.ENGSTRUCT.2022.114357

[29] "Iranian National Building Code. Design Loads for Buildings–Part 6", Office of National Building Regulations, Tehran, Iran, 2014.

[30] ASCE. Minimum design loads for buildings and other structures. Am Soc Civil Eng. 2013.

[31] No, Standard. "2800 V3 - Iranian Code of Practice for Seismic Resistant Design of Buildings", Building and Housing Research Center, Tehran, Iran, 2005.

[32] "Iranian National Building Code. Design of Steel Buildings–Part 10," Tehran, 2014.

[33] ANSI/AISC 360-16, Specification for Structural Steel Buildings, American Institute of Steel Construction, Chicago, Illinois, 2016.

[34] CSI (Computers and Structures Inc.). "SAP2000 v10 Integrated Finite Element Analysis and Design of Structures." CSI, Berkeley, 2004.

[35] Black C, Aiken ID, Makris N. Component testing, stability analysis, and characterization of buckling-restrained unbonded braces (TM). Pacific Earthquake Engineering Research Center, 2002.

[36] D. F.-M. Thesis, U. of Pavia, U. Pavia, U. Italy, and U. (2003). "Shape-memory alloy devices in earthquake engineering: mechanical properties, constitutive modelling and numerical simulations," compmech.unipv. it, 2003.

[37] Zareian F, Medina R. A practical method for proper modeling of structural damping in inelastic plane structural systems. Comput Struct. 2022; 88(1-2): 45–53.

[38] Engng E, Dyn S, Ibarra LF, Medina RA, Krawinkler H. Hysteretic models that incorporate strength and stiffness deterioration. Wiley Online Libr. 2005; 34(12): 1489–1511. https://doi.org/10. 1002/eqe.495